Proceedings of the 11th Brazilian Congress of Thermal Sciences and Engineering -- ENCIT 2006
Braz. Soc. of Mechanical Sciences and Engineering -- ABCM, Curitiba, Brazil, Dec. 5-8, 2006

Paper CIT06-0364

INVERSE DESIGN OF A ILLUMINATION SYSTEM HAVING NON-GRAY WALLS

Alexandre Seewald
Department of Mechanical Engineering
Federal University of Rio Grande do Sul
Porto Alegre, RS, Brazil
seewald@mecanica.ufrgs.br

Paulo Smith Schneider
Department of Mechanical Engineering
Federal University of Rio Grande do Sul
Porto Alegre, RS, Brazil
pss@mecanica.ufrgs.br

Francis Henrique Ramos França
Department of Mechanical Engineering
Federal University of Rio Grande do Sul
Porto Alegre, RS, Brazil
frfranca@mecanica.ufrgs.br

Abstract. This work applies the inverse analysis to an illumination design of a three-dimensional rectangular enclosure having non-gray walls. The problem consists of finding the luminous fluxes input on the light source elements, located on the top of the enclosure, to satisfy a prescribed uniform luminous flux on the design surface, located on the bottom surface. All the enclosure surfaces emit and reflect diffusively, but the hemispheric spectral emissivities are wavelength dependent in the visible region of the spectrum. The illumination design is inherently an inverse problem, in which the design surface is subjected to two conditions while the light sources are left unconstrained. Such problems are know to be ill-conditioned, and requires regularization methods to deal with the system of equation. In addition, the dependence of the surfaces emissivity on the wavelength lead to a system of non-linear equations. The ill-conditioned characteristics of the system of equations are tackled by the TSVD (Truncated Singular Value Decomposition) regularization method, while an iterative procedures is proposed to deal with the non-linearity of the equations. This work considers two design cases: one in which the light source elements cover the entire top surface; and one in which a reduced number of light sources are considered, a more practical solution. In both cases, the proposed inverse design is capable of providing a solution that satisfies the prescribed luminous flux on the design surface within average and maximum errors less than 2,0 and 10%, respectively.

Keywords. Inverse analysis, illumination design, non-gray surfaces, radiation exchanges, regularization methods

1. Introduction

A large variety of environmental control and industrial processes require the specification of the illumination level on a certain working area. Examples include plant growth as well as human and industrial activities. The designer must then specify the locations and power inputs of the light sources so that the required illumination flux is achieved. This problem usually involves a trial-and-error approach, in which the light sources are specified and calculations are run to verify if the required illumination is achieved. If not, another configuration is attempted, until the resulting illumination is satisfactory. This trial-and-error procedure may require many steps, since when an unsatisfactory result is obtained it is not clear which direction to take next, due to the complexity and non-linearity of the illumination relations. The illumination inverse design is an alternative procedure, from which the light sources configurations are directly found from the specified illumination flux.

The methods for the design of artificial lighting of environments were first established at the beginning of the 20th century. The luminous flux on a given working area is not only dependent on the power of the light sources, but also on the absorbing and reflecting effect of the remaining surfaces of the enclosure. The methods allowed the calculation of light radiation exchanges as well as for the characterization of the light sources behavior. In addition, many studies have been carried out to provide recommending lighting for the many possible applications, from human and industrial activities to plants growth (Boast, 1953; Mark, 2000). In general, not only the intensity of light (luminous flux intensity) is specified, but its uniformity.

The first works to deal with the illumination design were presented by Harrison and Anderson (1916 and 1920), who proposed an experimental procedure, the lumen method, in which the luminous flux on a working plane was determined from a combination of a series of proposed assembling of punctual and continuous light sources. In the 1940's, Moon (1941) and Moon and Spencer (1946a, 1946b) proposed the interreflection method for the design of

three-dimensional rectangular enclosures having any aspect ratio and being formed by diffuse surfaces. The method presented the advantage of allowing the calculation of the brightness of a surface, accounting for the reflection of light.

The advances in the field thermal radiation in the past century led to many analytical and computational tools that can be readily applied to illumination analysis, since light itself and thermal radiation in the visible region of the spectrum are essentially the same phenomenon. The sole difference is that the thermal radiation flux must be converted into luminous flux, accounting for the photopic luminous efficacy of the human eye. Schneider and França (2004) presented the application of the inverse analysis to the illumination design of an enclosure in which an uniform luminous flux was imposed on a working surface of the enclosure, the *design surface*. The work showed that such surfaces were constrained by two boundary conditions: the specified luminous flux and the luminous emissive power, which is zero. In the analysis, the luminous power required on the light sources were found directly from the two conditions imposed on the design surfaces, without involving the trial-and-error solution of the conventional techniques. However, as typical of inverse analysis, the formulation resulted in an ill-conditioned system of equations, which requires special solution techniques, such as the regularization methods (Hansen, 1998). A comprehensive review of inverse design involving radiative exchanges in enclosures was presented in França et al. (2003).

This paper aims at extending the analysis presented in Schneider and França (2004) to include surfaces that are non-gray. In such a case, the system of equations is non-linear in addition to the ill-posed characteristics of the inverse problem. The objective is to find the luminous power on the light sources located on the top surfaces of a three-dimensional enclosure that satisfy the specified uniform luminous flux on the design surface, located on the bottom of the enclosure. All the surfaces that form the enclosure are assumed to be diffuse. A zonal type formulation is applied for the discretization of the radiation exchanges. The ill-conditioned nature of the system is treated by means of the truncated singular value decomposition (TSVD). Results are presented for two cases: when the light sources cover the entire top surface; and when a reduced amount of light sources are considered, a more practical design proposition.

2. Physical and mathematical modeling

2.1 Luminous flux and thermal radiation

Incandescent lamps are common sources of light. Their main component is a resistance that reach temperatures around 3000 K under the passage of electric current. At such temperatures, a considerable amount of thermal radiation is emitted in the visible region of the wavelength spectrum, 0.4 μm ≤ λ ≤ 0.7 μm. The luminous flux, in units of lumens/m^2 or lux, can be related to the thermal radiation flux, in units of W/m^2, by means of the following relation:

$$q^{(l)} = CV_\lambda q^{(w)} \tag{1}$$

where $q^{(l)}$ and $q^{(w)}$ correspond respectively to the luminous flux (lumens/m^2) and to the thermal radiation flux (W/m^2) for a specific wavelength λ, C is a conversion factor constant, equal to 683 lumens/W, and V_λ is the so called photopic spectral luminous efficacy of the human eye, which takes into account the human eye sensitivity to the thermal radiation comprehended in the visible region of the spectrum, and is obtained by the following curve fitting:

$$V_\lambda = c_1 \exp(c_2 + c_3/\lambda + c_4 \ln(\lambda)) \tag{2}$$

where $c_1 = 9.77517\times10^{-1}$, $c_2 = 1.31695\times10^{3}$, $c_3 = -1.00004\times10^{5}$, $c_4 = -1.7989\times10^{2}$, and λ is in nm. According to the above relation, the spectral luminous efficacy peaks with a value of 1.0 for a thermal radiation in the wavelength of 0.555 μm, and then decay monotonically to zero as the lower and upper limits of the visible region, 0.4 μm and 0.7 μm, are approached. In general, a source of light is composed by radiation covering the entire range of the visible region. In such a case, Eq. (1) must be applied to each infinitesimal amount of the spectral energy and then be integrated in the visible spectrum. Such procedure will be demonstrated in the next section.

2.2 Radiation Exchanges in an Enclosure

Methods for the evaluation of radiation exchanges in an enclosure is well established in the literature (Siegel and Howell, 2002). To allow acceptable resolution in the variation of the radiative quantities, the surfaces are subdivided into sufficiently small elements, in which all thermal quantities can be assumed uniform. Next, the energy balance will be applied to each element j of the enclosure. The energy balance can take different forms as shown below:

$$q^{(w)}_{\lambda,o,j} = \varepsilon_{\lambda,j} e^{(w)}_{\lambda,b,j} + (1-\varepsilon_{\lambda,j}) q^{(w)}_{\lambda,i,j} \tag{3}$$

$$q^{(w)}_{\lambda,i,j} = \sum_k F_{j-k} q^{(w)}_{\lambda,o,k} \tag{4}$$

In the above equations, $q_{\lambda,o}^{(w)}$ is the spectral radiosity, in W/(m^{2}μm), which takes into account both emission and reflection; $q_{\lambda,i}^{(w)}$ is the spectral irradiation, in W/(m^{2}μm), corresponding to all radiation that arrives on the surface element; $e_{\lambda,b}^{(w)}$ is the spectral blackbody emissive power, in W/(m^{2}μm), which is given by Planck's blackbody distribution; ε_λ is the spectral emissivity; and F_{j-k} is the view factor between surface elements *j* and *k*. In the above equations the superscript (*w*) was used to indicate thermal energy. In a next step, the above equations are converted into luminous quantities. To accomplish this, it should be first noted that the thermal energy flux (W/m^2) in the wavelength λ centered in the interval *d*λ can be related to the spectral energy flux W/(m^{2}μm) by:

$$dq^{(w)} = q_\lambda^{(w)} d\lambda \tag{5}$$

The corresponding luminous flux (lumens) in the wavelength λ centered in the interval *d*λ follows from Eq. (1):

$$dq^{(l)} = CV_\lambda q_\lambda^{(w)} d\lambda = q_\lambda^{(l)} d\lambda \tag{6}$$

where $q_\lambda^{(l)}$ is the spectral luminous flux, in lumens/(m^{2}μm). Multiplying Eqs. (3) and (4) by CV_λ leads to:

$$q_{\lambda,o,j}^{(l)} = \varepsilon_{\lambda,j} e_{\lambda,b,j}^{(l)} + (1-\varepsilon_{\lambda,j}) q_{\lambda,i,j}^{(l)} \tag{7}$$

$$q_{\lambda,i,j}^{(l)} = \sum_k F_{j-k} q_{\lambda,o,k}^{(l)} \tag{8}$$

where $e_{\lambda,b,j}^{(l)}$ is the blackbody spectral luminous power, given by $e_{\lambda,b,j}^{(l)} = CV_\lambda e_{\lambda,b,j}^{(w)}$.

The above relations present the luminous energy balance for a given spectral wavelength λ. The complete solution requires the integration of the above relation for the entire spectral region that contains the visible region, that is 0.4 μm ≤ λ ≤ 0.7 μm. For gray surfaces, the spectral hemispherical emissivities $\varepsilon_{\lambda,j}$ can be readily removed from the integral, and the integration can be performed by simply introducing the total luminous quantities (Schneider and França, 2004). For non-gray surfaces, the spectrum domain can be divided into bands Δλ where the spectral hemispherical emissivities $\varepsilon_{\lambda,j}$ for the surfaces can be approximated by a constant value, represented by $\varepsilon_{\Delta\lambda,j}$. It follows that:

$$q_{\Delta\lambda,o,j}^{(l)} = \varepsilon_{\Delta\lambda,j} e_{\Delta\lambda,b,j}^{(l)} + (1-\varepsilon_{\Delta\lambda,j}) q_{\Delta\lambda,i,j}^{(l)} \tag{9}$$

$$q_{\Delta\lambda,i,j}^{(l)} = \sum_k F_{j-k} q_{\Delta\lambda,o,k}^{(l)} \tag{10}$$

where $q_{\Delta\lambda}^{(l)}$ is given by integration of $q_\lambda^{(l)}$ over band Δλ. Finally, the total luminous fluxes are obtained by the summation of the contribution of all bands, that is:

$$q_{o,j}^{(l)} = \sum_{\Delta\lambda} q_{\Delta\lambda,o,j}^{(l)} \tag{11}$$

$$q_{i,j}^{(l)} = \sum_{\Delta\lambda} q_{\Delta\lambda,i,j}^{(l)} \tag{12}$$

$$e_{b,j}^{(l)} = \sum_{\Delta\lambda} e_{\Delta\lambda,b,j}^{(l)} \tag{13}$$

where $q_o^{(l)}$ is the outgoing luminous flux, in lumens/m^2 or lux, which takes into account both emission and reflection; $q_i^{(l)}$ is the incident luminous flux, in lumens/m^2, the luminous energy that arrives from the light sources as well as from reflections from the side walls.

3. Problem definition

Figure 1 presents a schematic view of a three-dimensional enclosure, which is formed by surfaces that are diffuse but non-gray. The design surface is located on the bottom of the enclosure; the light sources are located on the top surface. The remaining of the enclosure is formed by walls that do not emit but reflect incident light. The length, width and height of the enclosure are designated by *L*, *W* and *H*, respectively. As depicted in Fig. 2, the enclosure is divided into finite-size square elements, $\Delta x = \Delta y = \Delta z$, in which the luminous energy balance will be applied. For designation of elements in the design surface, lamps and wall, indices *jd*, *jl* and *jw* will be used throughout this analysis.

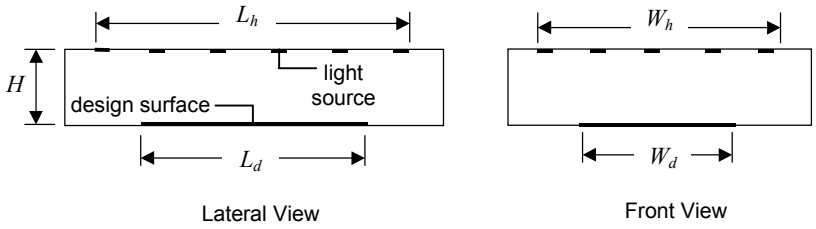

Figure 1. Three-dimensional rectangular enclosure.

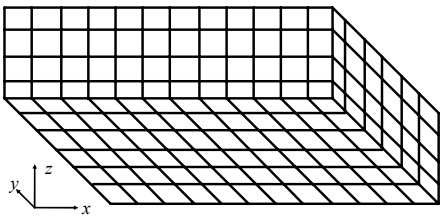

Figure 2. Division of the bottom and two side surfaces of the enclosure into finite size elements.

An uniform incident luminous flux, designated by $q^{(l)}_{specified}$, is specified on the design surface. In addition, no light is emitted from the design surface, so $e^{(l)}_{b,jd} = 0$. Therefore, two conditions are imposed on the design surface elements. For the elements on the wall, one single conditions is known, $e^{(l)}_{b,jw} = 0$, since they do not emit light. On the other hand, no condition is known for the light source elements. The conditions on the light sources are to be found from the two specifications ($q^{(l)}_{i,jd} = q^{(l)}_{specified}$ and $e^{(l)}_{b,jd} = 0$) on the design surface.

The conventional solution techniques deal with problems where only one condition (either the incident luminous flux or the blackbody luminous power) is imposed on each surface element. This leads to a system of equations on the unknown outgoing luminous flux of each element. This system is typically well-behaved and can be solved by any standard matrix inversion technique. Once the system is solved for the outgoing luminous fluxes, the conservation equations can be again applied to find the unknown condition (the incident luminous flux or the blackbody luminous power) of each surface element. Since the knowledge of one condition is required on each surface element, the conventional technique can tackle the illumination design only through a trial-and-error solution, in which the power luminous flux is guessed on each light source, and the solution is run to verify if the imposed incident luminous flux on the design surface is attained. Due to the nature of the problem, one should expect to make a large number of guesses to obtain an approximate solution.

The inverse design is an alternative technique to tackle the above problem without relying on a trial-and-error solution. Note that for a design surface element *jd*, since $e^{(l)}_{\Delta\lambda,b,jd} = 0$, the outgoing luminous flux in band $\Delta\lambda$ can be found directly from the specified incident luminous flux according to Eq. (9):

$$q^{(l)}_{\Delta\lambda,o,jd} = (1 - \varepsilon_{\Delta\lambda,jd}) q^{(l)}_{\Delta\lambda,i,jd} \tag{14}$$

Writing the above equation in dimensionless form, one obtains:

$$Q_{\Delta\lambda,o,jd} = (1-\varepsilon_{\Delta\lambda,jd})Q_{\Delta\lambda,i,jd} \tag{15}$$

The dimensionless luminous flux is given by $Q = q^{(l)} / q^{(l)}_{i,specified}$, so that $Q_{i,jd} = 1.0$, where:

$$Q_{i,jd} = \sum_{\Delta\lambda} Q_{\Delta\lambda,i,jd} \tag{16}$$

Next, Eqs. (9) and (10) are combined and applied to each design surface element *jd* (with $e^{(l)}_{\Delta\lambda,b,jd} = 0$) and rearranged to form a system of equations for the dimensionless outgoing luminous flux on the light source elements $Q_{\Delta\lambda,o,jl}$:

$$\sum_{jl} F_{jd-jl} Q_{\Delta\lambda,o,jl} = \frac{Q_{\Delta\lambda,o,jd}}{(1-\varepsilon_{\Delta\lambda,j})} - \sum_{jw} F_{jd-jw} Q_{\Delta\lambda,o,jw} \tag{17}$$

Note that in the above equation, the first term on the right-hand side is known. The outgoing luminous fluxes on the wall elements, $Q_{\Delta\lambda,o,jw}$, are unknown, so an additional relation is imposed by applying Eqs. (9) and (10) to these elements with the condition that $e^{(l)}_{\Delta\lambda,b,jw} = 0$. It follows that:

$$Q_{\Delta\lambda,o,jw} = (1-\varepsilon_{\Delta\lambda,jw})\left(\sum_{jd} F_{jw-jd} Q_{\Delta\lambda,o,jd} + \sum_{jl} F_{jw-jl} Q_{\Delta\lambda,o,jl} + \sum_{jw-jw'} F_{jw-jw'} Q_{\Delta\lambda,o,jw'} \right) \tag{18}$$

The last term arises from the fact that, as seen in Fig. 1, two walls element *jw* and *jw*' can "see" each other, in which case the view factor is not zero. Finally, the set of equations become complete arranging Eqs. (9) and (10) for each light source element *jl*:

$$E_{\Delta\lambda,b,jl} = \frac{1}{\varepsilon_{\Delta\lambda,jl}} \left(Q_{\Delta\lambda,o,jl} - \sum_{jd} F_{jl-jd} Q_{\Delta\lambda,o,jd} - \sum_{jw} F_{jl-jw} Q_{\Delta\lambda,o,jw} \right) \tag{19}$$

where $E_{\Delta\lambda,b,jl} = e_{\Delta\lambda,b,jl} / q^{(l)}_{i,specified}$ is the dimensionless emissive luminous power of light source element *jl* in band $\Delta\lambda$.

4. Solution procedure

For the illumination inverse design of enclosure having non-gray surfaces, an important difficulty arises in that only the total incident luminous flux on the design surface is known, but not its value on each band $\Delta\lambda$. To allow the application of the inverse design technique, the incident luminous in each band is first guessed by assuming that the same amount of luminous energy is distributed in each band $\Delta\lambda$, that is:

$$Q_{\Delta\lambda,i,jd} = \frac{Q_{i,jd}}{N_{\Delta\lambda}} \tag{20}$$

where $N_{\Delta\lambda}$ is the number of bands.

At this point, the approach proposed in Schneider and França (2004) for the entire visible wavelength region can be applied for each band $\Delta\lambda$. The outgoing luminous flux on the elements located on the walls are initially neglected in Eq. (17). Therefore, the unknowns in Eq. (17) are only the outgoing luminous fluxes on the light source elements, $Q_{\Delta\lambda,o,jl}$. Once Eq. (17) is written for each of the *M* elements that form the design surface, a system with *M* equations will be formed. The unknowns are the outgoing radiative heat fluxes on the *N* light source elements. Therefore, one aspect of the inverse design arises: the number of equations and the number of unknowns are not necessarily the same, unless *M* = *N*. In addition, since the problem corresponds to a discrete form of an integral equation of the first-kind, the system of equations is ill-conditioned, which require the application regularization methods, like the Tikhonov method, the conjugate gradient, the truncated singular value decomposition (TSVD), the modified TSVD, among others. In this solution, the TSVD method is chosen, as will be discussed later on.

Although a system of equations can be assembled in such a way to include the equations for the elements on the walls, an aspect of interest in the aforementioned procedure is that the elements in the design surface, where two conditions are imposed, are directly linked to the light source elements, where no condition is imposed. Thus, the ill-

posed part of the problem is separated from the remaining of the problem, allowing an isolated application of the appropriate methods of solution of ill-posed system of equations.

The solution is achieved by means of the following procedure. First, the outgoing luminous flux on each design surface element *jd* is computed by means of Eq. (15). The outgoing luminous flux on each wall element, $Q_{\Delta\lambda,o,jw}$, is initially set equal to zero. Then, the system of equations formed by Eqs. (17) is solved for the outgoing radiative heat fluxes on the light sources, $Q_{\Delta\lambda,o,jl}$. Next, Eq. (18) is applied to each wall element *jw* to form a (well-conditioned) system of equations on the outgoing luminous flux on the wall elements, $Q_{\Delta\lambda,o,jw}$. Once this system is solved, the newly computed $Q_{\Delta\lambda,o,jw}$ are inserted into the system of equations formed by Eqs. (17), and the procedure is repeated until convergence is achieved. Finally, with the converged values of the outgoing luminous fluxes, Eq. (19) is applied to solve for $E_{\Delta\lambda,b,jl}$, the dimensionless emissive luminous power of the light source element *jl* in band Δλ.

However, the above solution is valid only for the guessed distribution of the luminous incident flux on the design surface for each band Δλ, as given by Eq. (20), but there is no guarantee that the distribution is correct. To improve the guess, the first step is to note that, for each light source element *jl*, $N_{\Delta\lambda}$ values of $E_{\Delta\lambda,b,jl}$ are obtained, one for each band Δλ. Solving for the temperature associated with each band, the temperatures will not be necessarily the same, which is clearly not consistent, since a single temperature has to be associated with each light source element. To correct this result, the total emissive luminous power of each light source element *jl* is computed from:

$$E_{b,jl} = \sum_{\Delta\lambda} E_{\Delta\lambda,b,jl} \tag{21}$$

and a single temperature of the light source element can be computed by finding the temperature that will lead to the total emissive luminous power given by the summation of Eq. (21). This temperature will be an energy-based average of the temperatures obtained for each band Δλ.

At this point of the solution, an average temperature for each light source is obtained. A forward solution can be run where the light sources temperatures is known and the condition of null emissive luminous power is imposed to the design surface and to the walls. The solution of this problem leads to the incident luminous flux on each design surface element for each band Δλ, indicated by $Q'_{i,jd}$, so that the total incident luminous flux obtained by this procedure is:

$$Q'_{i,jd} = \sum_{\Delta\lambda} Q'_{\Delta\lambda,i,jd} \tag{22}$$

Note that $Q'_{i,jd}$ is not necessarily equal to the imposed value, equal to 1.0, since it resulted from the distribution guessed by Eq. (20). So a new distribution of incident luminous energy in the bands can be proposed so that:

$$Q_{\Delta\lambda,i,jd} = \left(\frac{Q'_{\Delta\lambda,i,jd}}{Q'_{i,jd}} \right) Q_{i,jd} \tag{23}$$

The procedure is repeated until the distribution of the incident luminous flux in the bands for each design surface element does not vary any more.

4.1 Regularization of the system of equations

The procedure discussed above involves the solution of a system of linear equations on the outgoing luminous fluxes on the light sources, as formed by Eqs. (17), which can be represented by:

$$\mathbf{A} \cdot \mathbf{x} = \mathbf{b(x)} \tag{24}$$

where matrix **A** is formed by the view factors between the design surface and the light source elements, F_{jd-jl}; vector **x** represents the unknown outgoing luminous fluxes on the light sources, $Q_{\Delta\lambda,o,jl}$; and vector **b** contains the terms on the right-hand side of Eq. (17), which are dependent on **x**.

The system formed by Eqs. (17) is expected to present the characteristics of ill-posed problems. In general, the components of the exact solution vector **x** present steep oscillations between very large positive and negative numbers, and small perturbations cause a much amplified change in the solution. One solving an ill-posed problems should not aim at an exact solution, but rather to impose additional constraints to reduce the size (norm) of **x,** and achieve a smooth

solution. However, the greater the smoothness imposed on the solution is, the greater will be the residual. This is the basic idea behind any regularization method for the solution of ill-posed problems.

Among the regularization procedures, the truncated singular values decomposition (TSVD) is employed here. First, matrix **A** is decomposed into three matrices:

$$\mathbf{A} = \mathbf{U} \cdot \mathbf{W} \cdot \mathbf{V}^{\mathbf{T}} \tag{25}$$

where **U** and **V** are orthogonal matrices, and **W** is a diagonal matrix formed by the singular values w_j. As a consequence, the solution vector **x** can be computed by:

$$\mathbf{x} = \sum_{j=1}^{N} \left(\frac{b_k \cdot u_{kj}}{w_j} \right) \mathbf{v}_j \tag{26}$$

where N stands for the number of unknowns (in this case, the number of light source elements).

In ill-posed problems, the singular values w_j decay continuously to very small values. Since they appear in the denominator of Eq. (26), the components of **x** can present very large absolute numbers. However, the smaller the singular value w_j is, the closer the corresponding vector $\mathbf{v}_j$ is to the null-space of **A**. In other words, the terms related to the smaller singular values can be eliminated from Eq. (26) without introducing a large error into the solution. This is the main idea of the TSVD: only the terms related to the p-th largest singular values are kept in Eq. (26), instead of all N terms. The solution is the vector **x** with the smallest norm subjected to minimum deviation $\left|\mathbf{A} \cdot \mathbf{x} - \mathbf{b}\right|$.

Another aspect of the inverse solution concerns the number of unknowns and the number of equations. The number of equations equals the number of unknowns only when the number of light source elements and the number of design surface elements are the same. In general, this is not always verified, as in the example cases to be shown later in this work. An important feature of the TSVD method is that it can also be applied to the situation where the numbers of unknowns and equations are not the same, as will be shown in the results section.

4.2 Verification of the solution

Due to the need of regularizing the system of equations, an exact solution is not expected. The following procedure is used for the verification of the solution. After the inverse solution is run to convergence, a forward problem is solved where the dimensionless emissive luminous powers on the light source elements are known, from the inverse solution, and only the condition null emissive luminous power is imposed on the design surface and on the wall elements. The incident luminous flux on each element design surface *jd* is then calculated and compared to the specified heat flux by:

$$\gamma_{jd} = \left| \frac{Q_{specified} - Q_{i,jd}}{Q_{specified}} \right| \tag{27}$$

where $Q_{specified}$ is the specified dimensionless incident luminous flux, equal to 1.0, and $Q_{i,jd}$ is the incident luminous flux resulting from the emissive luminous powers on the light sources that were obtained from the inverse solution. Once γ_{jd} is calculated for each element *jd* in the design surface, the arithmetic average and the maximum errors γ_{avg} and $\gamma_{\max}$ can be readily found.

5. Results and discussion

The case considered in this work consists of a three-dimensional enclosure as shown in the schematic of Fig. 1. The aspect ratio of the enclosure is W/L = 0.8, and the dimensionless height is H/L = 0.2. The selection of the other dimensions of the enclosure will require a few considerations. First, the design surface ought not to cover the entire extension of the base, since the portions close to the corners would be mainly affected by the reflections from the side walls, not from the luminous radiation from the light source elements on the top surface. Therefore, the design surface dimensions are taken as L_d/L = 0.8 and W_d/L = 0.6. The locations of the light sources will be proposed later on.

For the design surface elements, the luminous emissive power is zero and the dimensionless incident luminous flux is $Q_{i,jd} = 1.0$; for the wall elements, the luminous emissive power is also zero; the light source elements are unconstrained. As an example case of the application of the methodology, the wavelength spectrum in the visible region is divided into three bands. The hemispherical emissivities and its dependence to the wavelength are shown in Fig. 3 for design, wall and light source elements. Considering that the light sources are formed by incandescent tungsten filaments, they can be modeled as gray surfaces having hemispherical emissivity ε_{jl} = 0.36. The problem is at this point completely defined unless for the location of the light source elements, which will be discussed next.

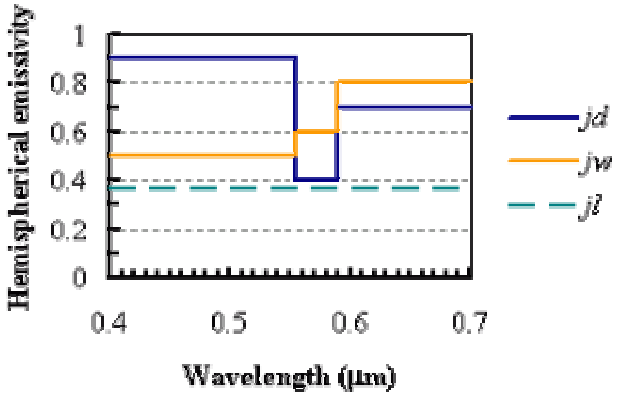

Figure 3. Spectral distribution of the hemispherical emissivity for the three types of surface elements. band b1 (0.40 μm < λ < 0.55 μm), band b2 (0.55 μm < λ < 0.59 μm), band b3 (0.59 μm < λ < 0.70 μm).

5.1 Case 1: light sources covering the entire top surface

To illustrate the inverse design, it is first considered that the light source elements cover the entire top surface. Figure 4 shows the locations of both the light source elements (circular dots) and the design surface elements (shaded area). Due to symmetry, indicated by the dashed lines, only a quarter of the domain is solved: $0 \le x/L \le 0.5$, $0 \le y/L \le 0.4$). One consequence of having the light sources covering the entire top surface is that the numbers of design surface and light source elements (indicated by M and N, respectively) are not the same. Selecting a grid size of $\Delta x/L = 1/30$, one finds $M = 108$ and $N = 180$. Thus, the system of equations formed by Eq. (17) is composed by $M = 108$ equations and $N = 180$ unknowns.

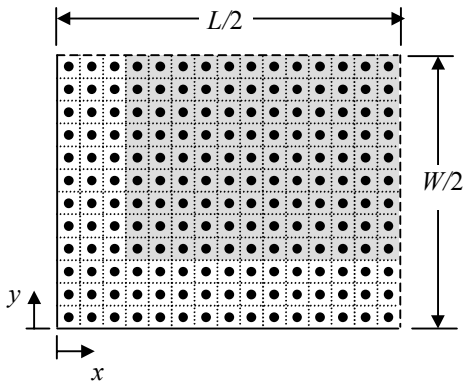

Figure 4. Locations of the design surface (shaded area) and light source elements (circular dots) in one quarter of the bottom and top surfaces for case 1: light sources covering the entire top surface. Dashed lines indicate symmetry.

The procedure presented in Section 4 is then applied to find the required net luminous flux and temperature of the light source elements. Figure 5 shows the singular values of matrix **A**, under the label Case 1. As typical of inverse design problems, the singular values w_j decay steadily to values that are as small as 10^{-10}. It should be noted that in the figure only the non-zero singular values are shown; for $j > M = 108$, all the singular values are zero. This indicates that the problem presents infinite exact solutions. To select the exact solution with the smallest norm, one needs only to apply the TSVD method to retain only the M first terms of the series of Eq. (26). In this case, it was observed that the components of vector **x** had very large absolute values, with alternating positive and negative signals, due the small singular values that arise in the denominator of the series terms. Since the components of vector **x** correspond to the outgoing luminous fluxes on the light sources, positive numbers, this exact solution has no physical meaning. However, the TSVD can be further explored to keep only the terms of the series corresponding to the p (< M) largest singular values. In this case, the obtained regularized solution will be no longer exact, but can present an acceptable behavior.

Figure 6 presents examples of regularized solutions for three different regularization parameters $p = 12$, 10 and 8. Solutions for $p \ge 13$ presented negative values for the emissive luminous power on some of the light sources, which is not physically acceptable. Solutions for $p = 11$, 9 and 6 were also obtained, but are not presented here since they did not bring additional features to those shown in Fig. 6. As can be seen in all cases, all the solutions present an oscillatory

behavior that are in fact reminiscent of the steep oscillations of the smallest-norm exact solution (that is, for $p = M = 108$). In general, the smaller the value p is, the smoother the solution will be, although at the expense of presenting a larger error. This can be verified in Table 1, which presents the maximum and average errors for different values of p, as defined in Section 4.2, as well the minimum singular value retained in the series of Eq. (26), $w_{j,\min}$.

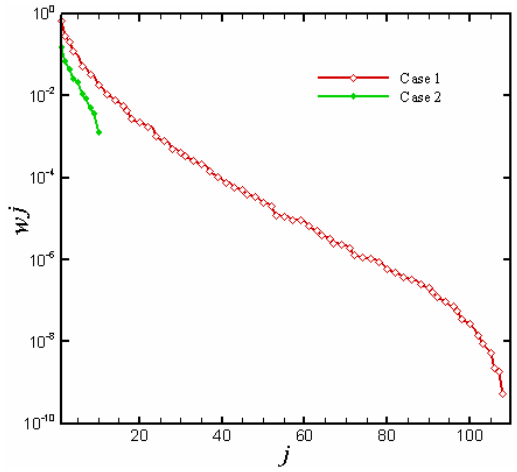

Fig. 5 – Singular values of matrix **A**: cases 1 and 2.

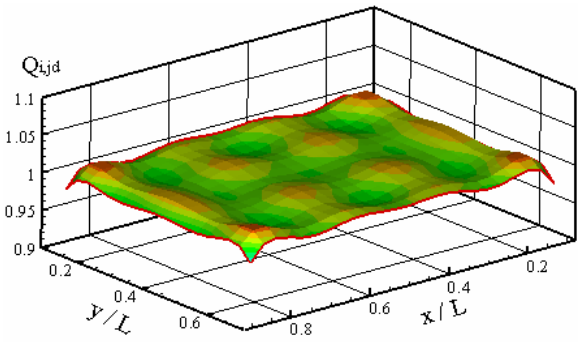

(a)

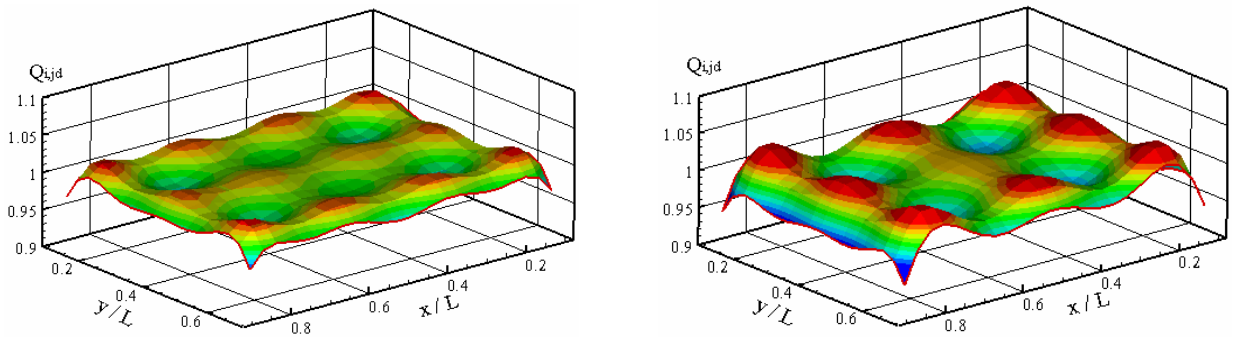

(b) (c)

Fig. 6 – Incident luminous flux distribution on the design surface for different regularization parameters p: (a) $p = 12$; (b) $p = 10$; (c) $p = 8$. Case 1.

Table 1 – Minimum singular value and inverse solution errors for different regularization parameters p.

p	$w_{j,\min}$	γ_{avg} (%)	γ_{max} (%)
12	1.1154×10^{-2}	0.4353	2.1692
10	1.7734×10^{-2}	0.7173	3.2396
8	3.3388×10^{-2}	1.3182	5.5417

5.2 Case 2: reduced number of light sources

The solutions obtained and discussed in the previous section illustrate the typical fact that the inverse design technique can lead to a number of approximate solutions, where the final selection can take into account the accuracy and practicality of the solutions. One aspect of the light source configuration of Fig. 4 is that a very large number of independent light sources are being required (that is, 4 × 180 = 720 elements for the entire enclosure), which is not practical. The designer will probably be much more interested on having a smaller amount of heat sources. For that matter, the previously selected solution (for p = 12) provide a hint towards this goal. Figure 7 illustrates a design where ten light sources are distributed on the entire top surface. Note that as expected the solution is symmetrical for each quarter of the domain. The locations of the light sources were proposed to approximately coincide with the points of maximum luminous fluxes for the solution with p = 12.

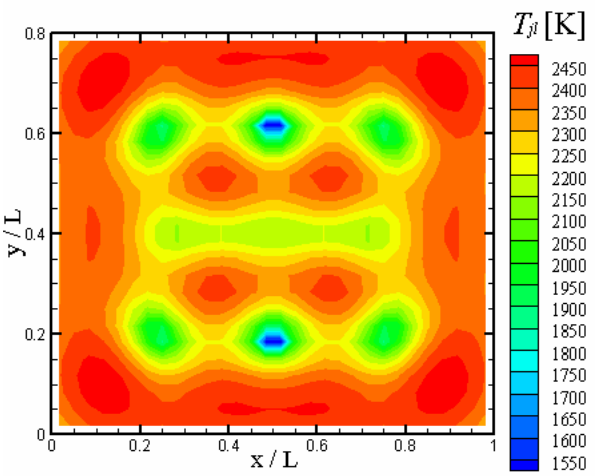

Fig. 7 – Required lamp filament temperature distribution on the top surface for the solution with p = 12. Case 1.

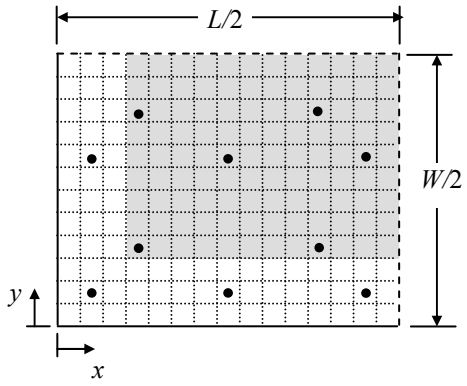

Fig. 7 – Locations of the design surface (shaded area) and light source elements (circular dots) in one quarter of the bottom and top surfaces for case 2: reduced number of light sources. Dashed lines indicate symmetry.

Since the number of elements on the design remains the same, M = 108, and the number of light sources is N = 10, the problem is overspecified: the number of equations M is larger than that of unknowns. It is well known that such a problem can only be solved with some approximation. Figure 5 presents the singular values of matrix **A** for this case, under the label of Case 2. As seen, the ten singular values decay to a value in the order of 10^{-3}. Keeping all the singular values in the series of Eq. (26) provides the smallest norm vector **x** that leads to the smallest norm $|\mathbf{A}\cdot\mathbf{x}-\mathbf{b}|$. The solution for p = 4 is shown in Table 2, which indicates the net luminous flux ($Q_{r,jl} = Q_{o,jl} - Q_{i,jl}$) and the temperature on each element shown in Fig. 7. In the table, the location of the light sources are indicated by indices i and j to designate the position in x and y directions, respectively. The luminous flux on the design surface is shown in Fig. 8. As seen the solution is within the interval -0.90 < $Q_{i,jd}$ < -1.10: the maximum and average error of the solution are 9.9783 % and 2.9458 %. If an error less than 10.0 % is acceptable, then the proposed solution is acceptable. Otherwise a larger number of singular values should be considered, until the solution start generating negative emissive power for light sources. Note that better solutions can be also achieved by the choice of other locations of the light sources.

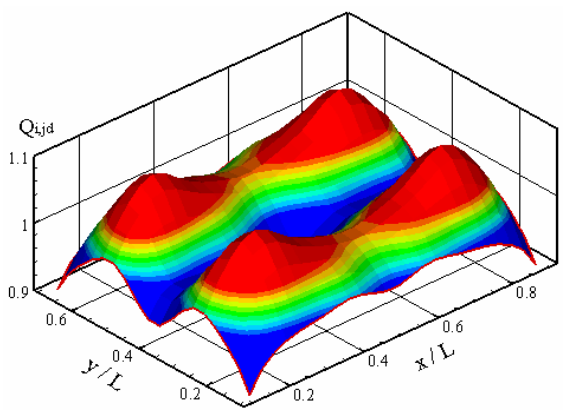

Fig. 8 – Dimensionless incident luminous flux on the design surface for the solution in case 2.

Table 2 – Required dimensionless net luminous on the light source elements for case 2.

jl	i	j	$Q_{r,jl}$	T_{jl} (K)	jl	i	j	$Q_{r,jl}$	T_{jl} (K)
1	2	2	12.8992	2978.17	6	8	8	35.7926	3378.41
2	2	8	18.6702	3111.76	7	12	4	22.2477	3179.28
3	4	4	26.7419	3253.13	8	12	10	17.0751	3078.80
4	4	10	23.2914	3197.36	9	14	2	13.5647	2996.33
5	8	2	23.2046	3195.99	10	14	8	14.0683	3009.22

Figure 9 shows the amount of energy in each of the three bands shown in Fig. 3. The sum of the energy in each band leads to the total incident irradiation of Fig. 8. Incandescent light sources filaments with temperatures in the order of 3000 K (see Table 2) have a luminous efficiency of about 5%. In this temperature level, most of the thermal radiation is concentrated in the infrared region ($\lambda > 0{,}70\mu m$). Therefore, band b3 ($0.59\mu m < \lambda < 0.70\mu m$), located in the larger wavelength region of the visible light interval, and closer to infrared region, contributes with the greater amount of energy. It follows that the contribution of band b2 ($0.55\mu m < \lambda < 0.59\mu m$) is also more significant than band 1 ($0.40\mu m < \lambda < 0.55\mu m$), despite occupying a smaller region of the spectrum.

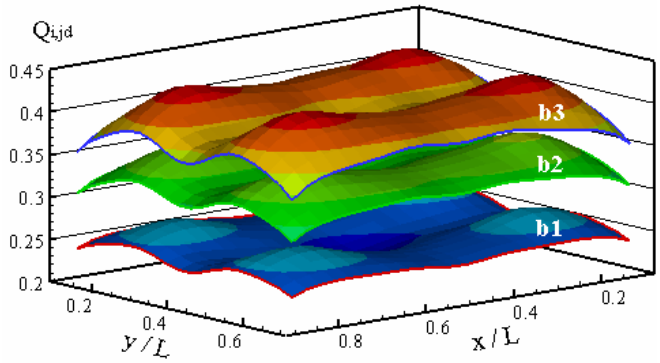

Fig. 9 – Dimensionless incident luminous flux for each spectral band considered for the design surface. Case 2.

All the above solutions involved a discretization of the spatial domain such that $\Delta x/L = 1/30$, which proved to be sufficiently small to guarantee grid independence. It should be pointed that, for greater generality, all the results were presented in dimensionless form, but conversion dimensional terms should be straightforward. For instance, the luminous power (in lumens) on each light source element of Table 2 can be determined as $Q_{r,jl} \cdot q^{(l)}_{specified} \cdot (\Delta x)^2$. Convergence with respect to the correction of the incident energy in the bands was achieved for all cases with four iterations, leading to a maximum variation of 10^{-6} between the results of the two last steps.

6. Conclusions

This work considered an inverse design problem of a non-gray enclosure in which the luminous fluxes on the light source elements were determined to satisfy the specified uniform incident luminous flux on the design surface. The numerical discretization of the problem led to an ill-conditioned system of non-linear equations. Ill-conditioned systems of equations require the application of regularization methods to recover physically acceptable solutions. In this work, it was employed the truncated singular valued decomposition (TSVD), which eliminates the linear combinations related to the smallest singular values of the system, keeping only the p largest ones. The non-linearity of the problem arose from the surfaces being non-gray, in which case the amount of energy in the spectral bands that cover the visible wavelength region is unknown.

The problem was formulated from the application of the luminous energy conservation in all the bands where the spectral emissivities could be assumed uniform. The example case consisted of three bands. The proposed procedure set a system of equations relating the design surface elements directly to the light source elements, calculating the outgoing luminous fluxes on the wall elements from the conditions of the previous iterative step. The unknown distribution of the incident energy on the design surface in the spectral bands were initially guessed, and then the inverse solution was run to find an average temperature on the light sources, from which a new distribution of the incident energy were used as a new input, repeating the process until convergence was reached. In most cases, four steps were enough to assure convergence within a relative error of 10^{-6}.

Two design cases were studied. In case 1, it was considered that the light source elements covered the entire top surface. The TSVD method was applied to find the solution for different regularization parameters, resulting in a few solutions that were evaluated according to physical requirements and the error of the solution. In case 2, it was proposed an inverse design in which only ten light source elements were set on the top surface (case 2). Despite the problem becoming overspecified, it was possible to obtain a solution more practical than having light sources covering the entire top surface, and still presenting an average and a maximum error less than 2.0 % and 10.0 %, respectively. It would be very difficult to arrive at such a solution by a trial-and-error procedure of the conventional forward technique.

7. Acknowledgments

The authors thank CAPES (Brazil) for the support under the program CAPES/UT-AUSTIN, No. 06/02.

8. References

Boast W.B, 1953, *Illumination Engineering*, McGraw-Hill, New York..

França, F., Howell, J., Ezekoye, O., and Morales, J. C., 2003, "Inverse Design of Thermal Systems," *Advances in Heat Transfer*, J. P. Hartnett and J. P. Irvine, eds., 36, Elsevier, pp. 1-110.

Hansen, P. C., 1990, *Truncated SVD Solutions to Discrete Ill-Posed Problems With Ill-Determined Numerical Rank*, SIAM J. Sci. Statist. Comput., 11, pp. 503-518.

Harrison, W. and Anderson, E. A., 1916, "Illumination Efficiencies as Determinated in an Experimental Room," *Trans. Illum. Eng. Soc*., **11**, pp 67-91.

Harrison W. and Anderson E.A., 1920, Coefficients of Utilization, *Trans. Illum. Eng. Soc*., **15**, pp 97-123.

Mark, S., 2000, *The IESNA Lighting Handbook*, Illuminating Engineering Society of North America, New York.

Moon P., 1941, "Interreflections in Rooms," *J. Optical Soc. Am*., **31**, pp 374-382.

Moon, P., and Spencer, D. E., 1946a, "Light Distribution in Rooms," J. Franklin Inst., **242**, pp 111-141.

Moon, P., and Spencer, D. E., 1946b, "Light Design by the Interreflection Method," *J. Franklin Inst*., **242**, pp 465-501.

Schneider, P. S., and França, F. H. R, 2004, "Inverse Analysis Applied to an Illumination Design", *Proceedings of the 10th Brazilian Congress of Thermal Sciences and Engineering*, Rio de Janeiro, Brazil.

Siegel, R., and Howell, J. R., 2002, *Thermal Radiation Heat Transfer*, 4th Ed. Hemisphere Publishing Corporation, Washington.

9. Copyright notice